

Influence of needle geometry on mechanical properties of 3D printed microneedle arrays

Martin Cseh^{1,2}, Gábor Katona¹, Ildikó Csóka¹

¹University of Szeged, Institute of Pharmaceutical Technology and Regulatory Affairs, Eötvös str. 6., H-6720 Szeged, Hungary

²University of Szeged, Center of Excellence for Interdisciplinary Research, Development and Innovation, 3D Center, Tisza Lajos blvd. 107., H-6725, Szeged, Hungary

Introduction

Microneedles have been extensively studied in both pharmaceutical and cosmetic sciences. These submillimeter structures tend to penetrate the stratum corneum and deliver active pharmaceutical ingredients with poor absorption properties. Before the appearance of desktop 3D printers' production costs of Microneedle Arrays (MNAs) was high. Additive manufacturing has become an affordable way to precisely produce these micron-scaled structures. (Li et al., 2022) Although stereolithography, a photopolymerization-based technology can provide precise, sharp needles, the cured polymer itself may not be mechanically stiff enough to penetrate the skin without breaking or bending which can cause unwanted complications during the application. This work intended to share the results of the mechanical analysis of different geometry based MNAs to determine the influence of these factors.

Materials and methods

High Temp V2 resin was obtained from Freedee Nyomdai Szolgáltató Művek Kft (Budapest, Hungary), Isopropyl alcohol was acquired from Molar Chemicals (Halásztelek, Hungary).

Shapr3D (Shapr3D, Budapest, Hungary) CAD software was used to design the 3D MNA models. MNAs were printed with a Form3 Low Force Stereolithography (LFS) printer (Formlabs, Somerville, Massachusetts, USA). Morphology studies of the samples were conducted on an Olympus DSX510 (Olympus Corporation, Shinjuku,

Tokyo, Japan.) 3D microscope. The mechanical properties were determined with a TA-XT Plus texture analyzer (Metron Kft, Budapest, Hungary).

Results and discussion

To determine the influence of needle geometry to the mechanical properties, 6 different geometries were designed. A cone-shaped needle served as control geometry. Triangle, square, pentagon, hexagon-based pyramids and a cut cylinder were also designed. The cone shaped needle had a 400 μm base and a nominal height of 1000 μm . A single needle with these parameters had 0.04 mm^3 volume. To be able to compare the influence of the different shapes the needle height and volume were fixed to 1000 μm and 0.04 mm^3 respectively.

The radiuses of the calculated circumcircles of the different shapes can be found in Table 1. The cut cylinder had also 400 μm base diameter and 1000 μm with a 50° side cut from the top (note: volume differs from the previously mentioned shapes). Each MNA consisted of 3x3 needles on a carrier plate (dimensions: 7 mm x 7 mm x 1 mm). 3D microscopic reconstructions of the printed MNAs can be found in Figure 1.

The printed needles were post-processed with the protocol provided by the manufacturer: 6' washing in isopropyl alcohol, drying, then 120' UV and 80 °C. The MNAs were then put on a 10 mm diameter probe on the TA-XT texture analyzer and measured. The force was parallelly applied to the needles and measured depending on the immersing distance (max distance was 1 mm). Results of the texture analyzer showed minor differences between the conical and pyramid shaped needles. The force

vs distance curves were almost identical in every measurement. The needles in these samples did not break, only bent but had similar bending fail patterns. A noticeable difference was observed on the cut cylinder samples compared to the aforementioned shapes.

Table 1. Parameters of the differently shaped needles

Needle shape	Base (circumcircle*) diameter [μm]	Height [μm]	Volume [mm^3]
Cone	400	1000	0.04
Triangle pyramid*	607.8	1000	0.04
Square pyramid*	489.8	1000	0.04
Pentagon pyramid*	449.4	1000	0.04
Hexagon pyramid*	429.8	1000	0.04
Cut cylinder*	400	1000	0.10

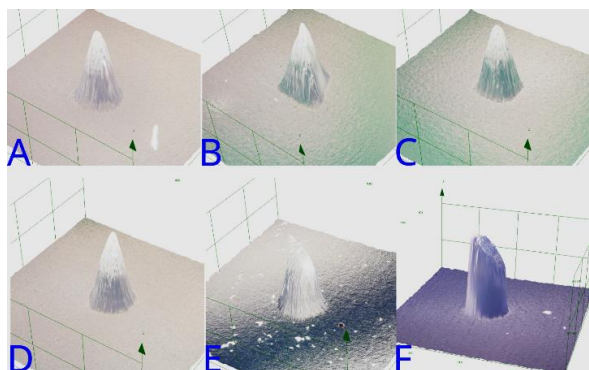


Fig. 1. Reconstructed 3D models of the printed samples with different needle shape: cone (A), triangle pyramid (B), square pyramid (C), pentagon pyramid (D), hexagon pyramid (E) and cut cylinder (F).

This geometry was able to withstand higher forces at the beginning compared to the conical and pyramid shapes but started to fail earlier. In this case the samples cracked which was well observable on the curves as small dents which were not present at the measurement of the other shaped needles. Visualized results can be seen on Figure 2. The average reactive forces measured on each sample at 0.8 mm immersion distance are shown on Table 2.

Table 2. Reactive forces measured at 0.8 mm immersion

Needle shape	Measured force average at 0.8 mm immerse [N] (Higher is better)
Cone	38.04
Triangle pyramid	36.08
Square pyramid	37.03
Pentagon pyramid	36.05
Hexagon pyramid	37.88
Cut cylinder	35.19

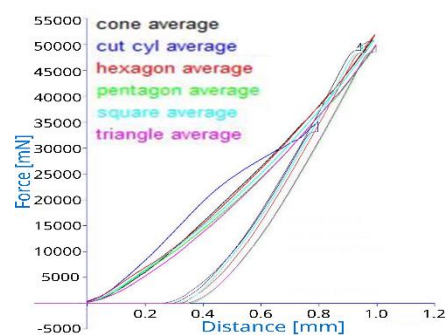


Fig. 2. Mechanical analysis average curves of the different needle geometries.

Conclusion

Based on the data gathered from the experiments, it can be concluded that the different base geometries slightly influenced the mechanical strength of the MNs. In practical manner there is no relevant difference between the conical and the pyramid shaped needles. The “cut cylinder” sample held bigger forces in the lower immerse distance region but failed earlier. It is hypothesized that this phenomenon happened due to the asymmetrical shape of the needle. The cylinder shape itself could be responsible for the higher strength in the lower region but the asymmetric head started to tilt the needle and instead of compression damage it broke after the necessary force applied.

Acknowledgement: This work was supported by Project no. TKP2021-EGA-32 implemented with support provided by the Ministry of Innovation and Technology of Hungary from the National Research, Development, and Innovation Fund, financed under the TKP2021-EGA funding scheme

References

- Li, R., Zhang, L., Jiang, X., Li, L., Wu, S., Yuan, X., Cheng, H., Jiang, X., & Gou, M. (2022). 3D-printed microneedle arrays for drug delivery. *J. Control. Release*, *350*, 933–948. <https://doi.org/10.1016/j.jconrel.2022.08.022>
- Maced. pharm. bull., **69** (Suppl 1) 41 - 42 (2023)